Chemistry Research Journal, 2021, 6(3):16-27

Available online www.chemrj.org

Research Article

ISSN: 2455-8990
CODEN(USA): CRJHA5

Kinetics and Thermodynamic Study of Reduction of Chromium(VI) by Dissolved Organic Matter (DOM) obtained from Groundnut Husk and Saw Dust

Boniface T. Iorhuna*[1], Raymond A. Wuana[2], Stephen G. Yiase[3], Timothy T. Awuhe[4], Olubunmi A. Ogundiran[1], Ernest I.[1]

1Taraba State University, chemistry Department, Jalingo, Taraba State, NG,
[2]Federal University of Agriculture Makurdi, Chemistry Department, Makurdi, Benue State, NG
[3]Benue State University, chemistry Department, Makurdi, Benue State, NG,
[4]Federal Polytechnic of Oil and Gas, Bonny Island, Rivers State, NG

Abstract A kinetic and thermodynamic approach was used to study the reduction of Cr^{6+} in aqueous phase by dissolved organic matter (DOM) obtained from ground nut husk (GH) and saw dust (SD). These reactions were monitored using UV-visible spectrophotometry. The reaction products were identified as Cr^{3+}, DOM was confirmed by its UV absorption, having λ_{max} of 256 nm and 250 nm for DOM(GH) and DOM(SD), its infrared spectra, with major absorption bands in the regions of 2500 – 3500 cm^{-1} and 650 - 770 cm^{-1} (O-H stretching and out of plane bending groups), 2500 – 3500 cm^{-1}, 1350 – 1470 cm^{-1} and 690 – 900 cm^{-1} (C–H stretching, deformation, and bending and ring puckering respectively), 1650 – 1800 cm^{-1} (C=O stretching of COOH), 1620 – 1680 cm^{-1} (alkene/aromatic C=C stretching), 970 – 1250 cm^{-1} (C–O stretching of alcohols/phenols) 880 – 995 cm^{-1} and 1395 – 1440 cm^{-1} (=C–H out of plane bending/C-O-H bending) respectively as well as scanning electron microscopy, SEM. The rate of reduction of Cr(VI) increased with mass/volume percent of DOM {the increment was higher with DOM(SD)}, decreased with increase in pH and independent of the ionic strength. Reaction rate also increased with temperature but having rate at 273 K comparable to that at 303 - 308 K. The activation energy (E_a), enthalpy change (ΔH), and entropy change (ΔS) were determined as; 83.31 $kJmol^{-1}$ and 72.44 $kJmol^{-1}$, -80.85 $kJmol^{-1}$ and -69.95 $kJmol^{-1}$, and -32.59 $Jmol^{-1}K^{-1}$ and -65.26 $Jmol^{-1}K^{-1}$ for $Cr_2O_7^{2-}$/DOM(GH) and $Cr_2O_7^{2-}$/DOM(SD) respectively.

Keywords Reduction, Chromium(VI), Kinetics, Thermodynamic, Dissolved organic matter

Introduction

Chromium and its compounds are toxic substances introduced into natural water from a variety of industrial wastes. The major sources are from leather tanning, textile dyeing, electroplating, municipal refuse incineration, ferrochromium production, chrome ore refining, sewage sludge incineration, petroleum refining cooling towers, metal finishing industries, e.t.c., which cause severe environmental and public health problems. Although Cr is an essential element for humans, the hexavalent form of chromium is considered to be a group "A" human carcinogen because of its mutagenic and carcinogenic properties [1]. As such, the widespread presence of Cr in the environment poses a serious threat to human and animal welfare; it leads to liver damage, pulmonary congestion, causes skin irritation, resulting in ulcer formation [2]. Its concentration in industrial waste water ranges from 0.5 - 270,000

mgL^{-1}. The tolerance limit for the discharge of Cr(VI) into inland surface water is 0.1 mgL^{-1} and in potable water is 0.05 mgL^{-1} [1].

On a worldwide basis, the major chromium source in aquatic ecosystems is domestic waste water effluents (32.2 % of the total) [3]. The other major sources are metal manufacturing (25.6 %), ocean dumping of sewage (13.2 %), chemical manufacturing (9.3 %), smelting and refining of nonferrous metals (8.1 %), and atmospheric fallout (6.4 %) [4]. Annual anthropogenic input of chromium into water has been estimated to exceed anthropogenic input into the atmosphere [4].

The toxicity of Cr, however, is a function of its oxidation state. Cr(VI), which typically exists as the oxyanion chromate (CrO_4^{2-}), has a high solubility in soils and groundwater and, as a consequence, tends to be mobile in the environment. In contrast, the reduced form of Cr, Cr(III), has a limited hydroxide solubility and forms strong complexes with soil and water minerals [5]. While Cr(III) is relatively innocuous and immobile, Cr(VI) is actively transported into cells by the sulfate transport system where it is capable of causing damage to DNA as well as indirectly generating oxygen radicals.

Chemical developments and usage in the new millennium are now routinely utilizing the concept of "green chemistry" to meet the challenges of protecting the environment and human health while maintaining commercial viability, hence the choice of a particular analytical technique for toxic metal (particularly Cr) remediation should rather be one that is eco-friendly in the utilization of agents for such a process. Several techniques effectively lower Cr concentrations in aqueous solutions; coagulation/precipitation, reverse osmosis, ion exchange, and adsorption to mention a few. Coagulation and softening with metal ions such as aluminium and ferric salts require use of large-scale facilities for implementing water treatment. Reverse osmosis requires the use of membranes, which are expensive to maintain and replace, and ion exchange uses costly resins. Again, coagulation, reverse osmosis, and ion exchange require the treatment of reject stream for the ultimate disposal of Cr contaminants [6]. Unlike adsorption technique that is aimed at removing toxic metals from the aqueous solutions, reduction technology leave them in the medium but minimize their toxicity and mobility. At the same time, various agricultural and industrial wastes are found to litter the local environments especially within the areas in which such wastes are produced. Ground nut husks for instance, has been found to be non-decomposable (at least within a year or two) if disposed as such, and saw dusts which are produced at one point or the other and have been found to be of little or no use. The effect of organic matter obtained from these waste on the reduction of Cr(VI) may turn out to be a greener approach to the remediation of heavy metals.

Materials and Methods

Chemicals, reagents and apparatus

$K_2Cr_2O_7$ (JHD^{AR}), CrO_3 (LOBA^{AR} CHEMIE PVT Ltd), Cr_2O_3 (LOBA^{AR} CHEMIE PVT Ltd), HNO_3 (BDH^{AR}), $NaNO_3$ (Fenxichun^{AR}), H_2SO_4 (97 – 99 % assay, JHD^{AR}), O-phosphoric acid, H_3PO_4 (Fenxichun^{AR}), o-phenanthroline (Qualikems^{AR}), $FeSO_4 . 7H_2O$ (JHD^{AR}), $Fe(NH_4)_2(SO_4)_2 . 6H_2O$ (LOBA^{AR} CHEMIE PVT Ltd), saw dust, ground nut husk, distilled and deionised water, muffle furnace (NEY M-525), mechanical shaker (HY-2 Speed adjusting multipurpose vibrator), thermostatic water bath (Clifton unstirred bath model 92498), UV-visible spectrophotometer (Unico^R 2800P), pH meter (Hanna Instrument H19024), analytical balance (aeADAM PW 184, AE 437531), freeze dryer (Lyodry, Grande freeze dryer model), FTIR spectrophotometer (Agilant Technolologies, Cary 630 FTIR), Sieve (Cole Parmer-typed sieve of 0.80 mm mesh) and normal laboratory glasswares.

Determination of UV-visible spectrum of the chromium(VI) and chromium(III)

Solutions of the salts of CrO_3 and Cr_2O_3 were prepared (with 0.009 $molL^{-1}$) and the absorbances of the solutions taken in the wavelength range (300 - 850 nm) with a Unico^R 2800P UV-visible spectrophotometer [7]. The wavelengths of maximum absorption were obtained by plot of absorbances versus wavelengths.

Preparation and characterization of DOM from ground nut husk (GH) and sawdust (SD)

The waste materials were collected locally; sawdust from a local sawmill (along George Akume Road, International Market, Makurdi, Benue State-Nigeria) and ground nut husk from a ground nut peeling center (Jalingo, Taraba State-Nigeria). The saw dust was sieved with a Cole Parmer-typed sieve of 0.80 mm mesh in order to obtain a desirable size fraction. Then, the sieved saw dust was washed with distilled water to remove any residues or impurities such as ash and dust. Ground nut husk on the other hand were first washed with distil water, dried in an oven and grounded through the sieve to lower the surface area, followed by the procedure described above [8 and 9]. Subsequently, these were dried in an oven. After drying, the materials were pyrolysized (at < 350 ^{o}C for 20 min) in a furnace to obtain the biochar [8].

10 g each of the biochar obtained from ground nut husk and saw dust were suspended in a reaction vessel with deionized water, and agitated on a shaker at an average speed at room temperature for 24 hours (to reach an apparent equilibrium). The suspensions were then passed through a filter paper and a 0.2 μm membrane filter to obtain DOM [6]. The percentage mass/volume of DOM was analyzed by Walkley-Black titrimetric method [9 - 11].

In determining the chemical structure and functional groups involved in Cr reduction reaction, DOM samples (DOM(GH) and DOM(SD) containing a percentage mass/volume of carbon were analyzed. To achieve this, 300 mL of DOM samples each containing varying percentage mass/volume DOM were freeze-dried and analyzed. The functional groups were analyzed after freeze drying the DOM samples using FTIR, UV-visible spectrophotometer and scanning electron microscopy (SEM). The colours of the solutions used were also observed to see the changes that occur [6 and 12, 13].

Kinetic Studies

All rate measurements were made using Unico^{R} 2800P UV-visible spectrophotometer at the wavelengths of maximum absorptions. The reaction rates were monitored at the wavelength by noting the decrease in absorbances of the reaction mixtures with time. The results were interpreted based on the fact that, Beer's law is additive for a multi component sample, equations 1 and 2

$$(A)\lambda_1 = (\varepsilon_{Cr(VI)})\lambda_1 l C_{Cr(VI)} + (\varepsilon_{Cr(III)})\lambda_1 l C_{Cr(III)} \quad (1)$$

$$(A)\lambda_2 = (\varepsilon_{Cr(VI)})\lambda_2 l C_{Cr(VI)} + (\varepsilon_{Cr(III)})\lambda_2 l C_{Cr(III)} \quad (2)$$

where A is the absorbances of the mixtures, λ_1 and λ_2 are wavelengths at which the absorbances were measured, $\varepsilon_{Cr(VI)}$ and $\varepsilon_{Cr(III)}$ are the molar absorptivities, $C_{Cr(VI)}$ and $C_{Cr(III)}$ are the concentrations and l is the path length [13].

All kinetic measurements were made under pseudo-first order conditions with the concentration $Cr_2O_7^{2-}$ at least 60 times greater than that of DOM [7].

The pseudo-first order rate constants, k_{obs}, were obtained from the plots of $\ln(A_t\text{-}A_\infty/A_o\text{-}A_\infty)$ against time (where A_t, A_o and A_∞ are the absorbances of the reaction mixtures at times t, zero time and infinite time respectively). The temperature was kept constant at ambient (297 – 300 K), pH = 6 and I = 0.1 mol L^{-1}.

pH dependence studies

The pseudo first order rate constants, k_{pH} for the reduction reaction involving Cr(VI) and DOM were determined at pH in the range of 2 – 10 (using HNO_3 and NaOH), keeping other conditions constant.

Temperature dependence studies

The temperature dependence rate study for the reduction reaction involving Cr(VI) and DOM were carried out over the temperature range of 288 - 308 K and 273 K while keeping other conditions constant. Kinetic activation parameters (activation energy, E_a, entropy change, ΔS, and enthalpy change, ΔH) were obtained from Arrhenius and Eyring plots [14-16].

Ionic Strength Effect

The effect of ionic strength changes on the rate of reduction reaction involving Cr(VI) and DOM have been studied over the range of (0.001 - 0.021) molL^{-1} concentrations of $NaNO_3$ salt, keeping other conditions constant.

Results and Discussion

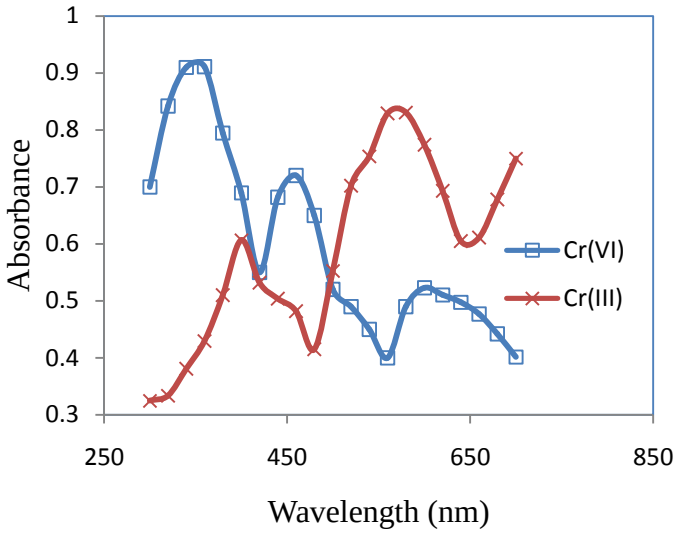

Figure 1: Determination of λ_{max} for Cr(VI) and Cr(III) ions

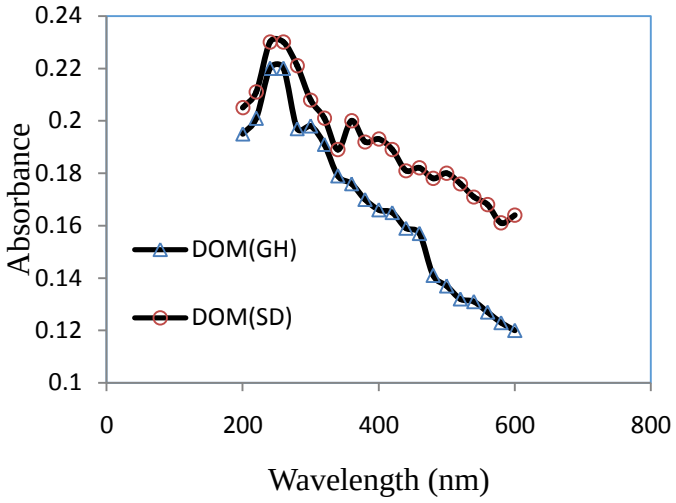

Figure 2: Determination of λ_{max} for the dissolved organic matter (DOM) from ground nut husk (GH) and saw dust (SD)

Spectra consideration of the solutions used

In Figure 1 above the bands correspond to the d – d transitions; the redistribution of electrons among orbitals that are mainly localized on the metal atoms or charge-transfer (CT) transitions involving the metal d-orbitals. Typically, the bands above 300 nm and below 850 nm, involve the motion of electrons from an essentially ligand-based orbital to an essentially metal-based, or vice versa. This makes charge to be transferred from one atom to another. In general, it is referred to as ligand – to – metal charge – transfer (LMCT). CT bands are observed if the energies of empty and filled ligand- and metal-centered orbitals are similar. It occurs within the visible or near UV region of the spectrum [8 and 14]. Thus the kinetic studies were done using UV-visible spectrophotometry and at the established wavelengths of maximum absorbances of the solutions used.

Characterization of the Dissolved Organic Matter, DOM samples

The DOM samples were characterised by measuring the content of their humic materials. In achieving this, 300 mL each from the DOM samples were freeze dried using a freeze drier, after which the DOM samples were characterised by FTIR, UV-visible spectrophotometer and SEM [6 and 12].

UV-visible and FTIR spectroscopy are powerful tools that can be used in the identification of complex (organic) compounds. These enable chemists to obtain absorption spectra of compounds that are a unique reflection of their molecular structures (including bands of humic materials) [17].

From the UV-visible spectra of these DOM samples (Figure 2 and Table 1), it can be seen that the wavelengths of maximum absorption were found as 250 nm DOM(SD) and 256 nm DOM(GH). In both cases, the UV-visible spectra have shown similarities in the peaks, similar results have been reported by Shie-Jie, *et al*, [18]. The UV-visible spectra data of the DOM samples were recorded in ethanol in the wavelength range 200 - 600 nm at ambient temperature (298 – 300 K), using a 1.0 cm quartz cell, reference was pure water. Samples were diluted to maintain the maximal response as reported by Shie-Jie, *et al*, [18].

The characteristic energy of a transition and the wavelength of radiations absorbed are properties of a group of atoms rather than of electrons themselves. The group of atoms producing such absorption is called a chromophore [19]. The electronic spectra data of humic materials have λ_{max} at 254 nm [20]. These UV-visible spectra data from the DOM samples might have been contributed by phenolic, aromatic carboxylic, and polycyclic aromatic compounds of the humins [18]. The bands may be attributed to $\pi \rightarrow \pi^*$ and $n \rightarrow \pi^*$ transitions [18 and 19].

The IR spectra of both DOM samples have been obtained (Figures 3 and 4), (Table 1 has the spectra data for these bands). They have a variety of bands typical of those for humic materials (humic and fulvic acids). The major absorption bands are found in the regions of 2500 – 3500 cm^{-1} and 650 - 770 cm^{-1} (O-H stretching and out of plane bending groups), 2500 – 3500 cm^{-1}, 1350 – 1470 cm^{-1} and 690 – 900 cm^{-1} (C–H stretching, deformation, and bending and ring puckering respectively), 1650 – 1800 cm^{-1} (C=O stretching of COOH), 1620 – 1680 cm^{-1} (alkene/aromatic C=C stretching), 970 – 1250 cm^{-1} (C–O stretching of alcohols/phenols), 880–995 cm^{-1} and 1395 – 1440 cm^{-1} (=C–H out of plane bending/C-O-H bending). These spectra evidently show predominance of OH and COOH groups which are the most characteristic features of humic materials. It is obvious that the IR results are in good agreement with the other characterization findings as reported by Helal, *et al*, [17], Shie-jie, *et al*, [18] and Silverstein, *et al*, [19].

Furthermore, Figures 5 and 6, showed the scanning electron microscopy, SEMs undertaken on the DOM samples that took part in the redox reactions. These can be seen to change in their surfaces after the DOM samples took part in the reduction reactions [6].

On the basis of the FTIR, UV-visible spectrophotometer and SEM analysis, it can be said that, those samples {obtained from ground nut husk (GH) and saw dust (SD)} contained DOM that also evidently reduced Cr(VI) to Cr(III) {as the colour changed from yellow Cr(VI) to green Cr(III) and there are changes on the SEMs before and after the reactions}. Also, the similarity of these absorption bands indicated that many similar structural and functional groups existed in the DOM from both agro wastes.

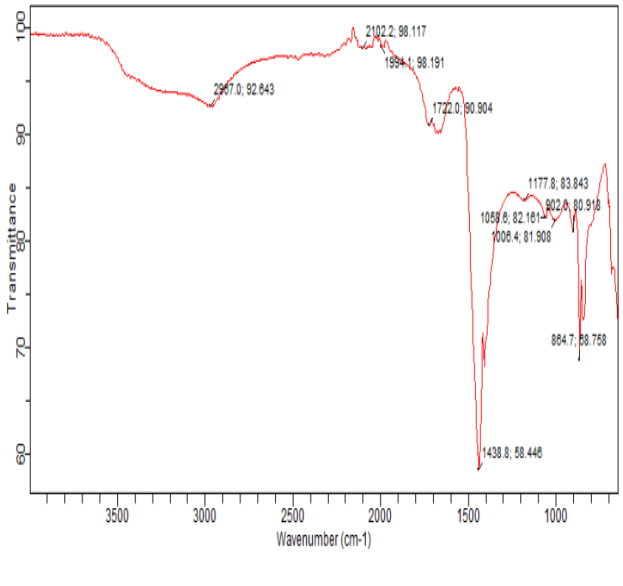

Figure 3: Infra-red spectrum of the DOM obtained from ground nut husk

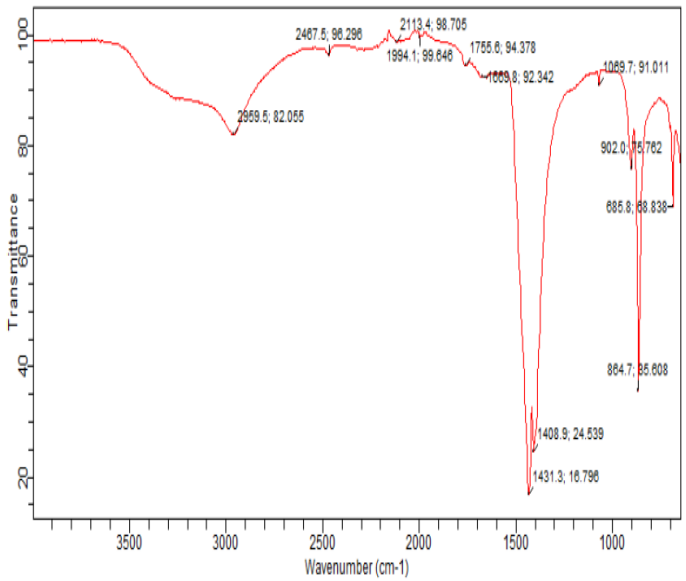

Figure 4: Infra-red spectrum of the DOM obtained from saw dust

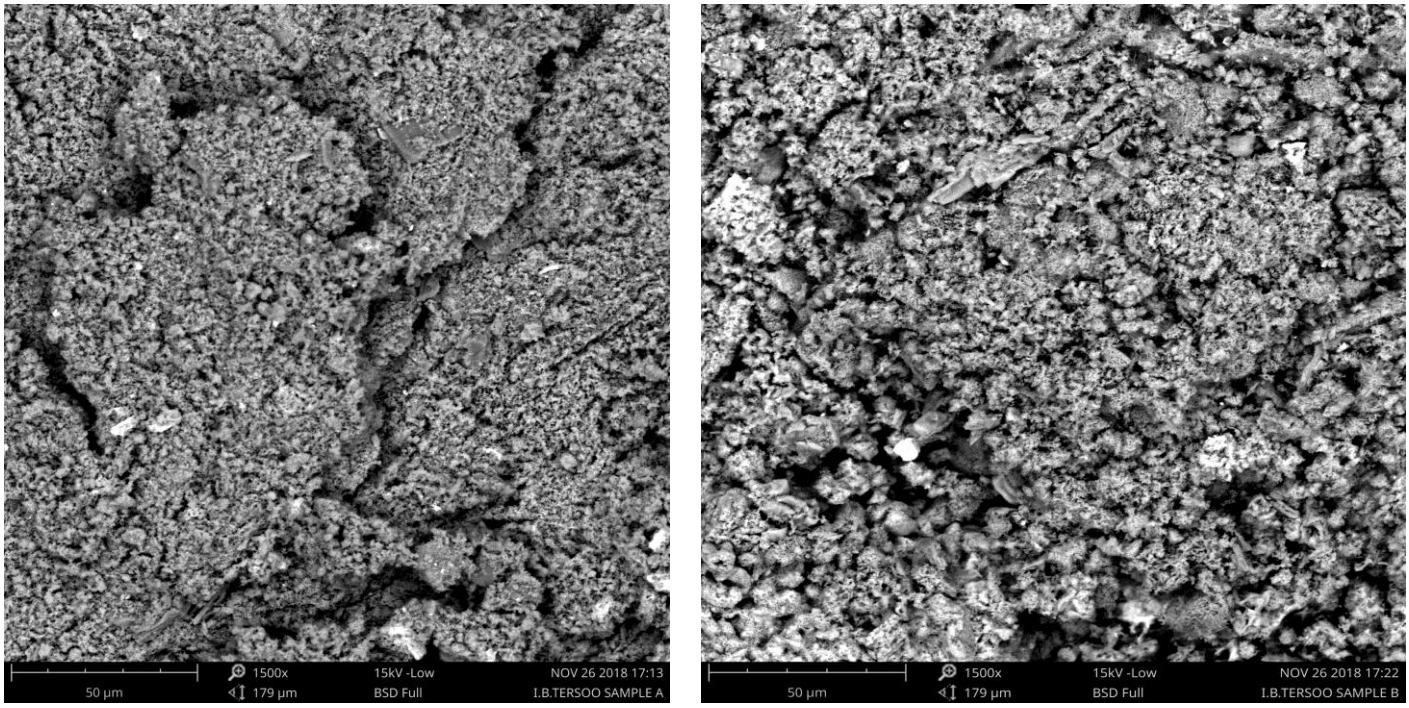

(a) **(b)**

Figures 5: The scanning electron microscopy, SEMs of the DOM samples before reduction reactions, (a) From ground nut husk and (b) From saw dust

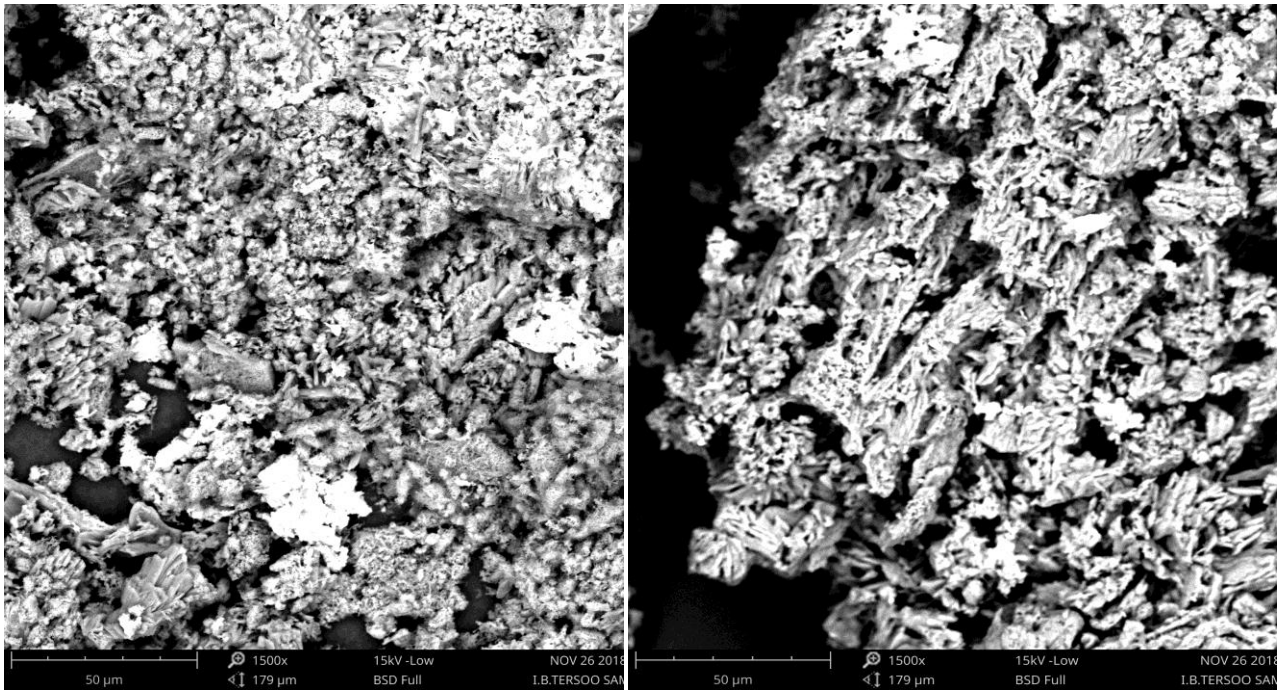

(c) **(d)**

Figures 6: The scanning electron microscopies, SEMs of the DOM samples after reduction reactions. (c) From ground nut husk and (d) From saw dust

Effect of the Initial Concentration on the Rate of Reaction

Ground nut husks and wood sawdust have been used as sources of biochar and/or organic matter, which have been seen to reduce Cr(VI) to Cr(III) [6]. The pseudo-first order plots for the reduction reactions involving $Cr_2O_7^{2-}$ ion with DOM(SD) and DOM(GH) are presented in Figures 7 and 8. Table 2 gives the k_{obs} values of these reactions and can be seen that, the reaction rates increased with percentage weights/volumes DOM, but has no observable reaction rate at very low volumes, these agree with the fact that, reactions proceed at faster rate when concentrations are high because of increased effective collisions resulting to faster rate of reaction [21]. Similarly, the effect of DOM on reduction reaction is higher with DOM(SD) compare with DOM(GH) as DOM(SD) found to have higher percentage weight/volume dissolved organic matter than DOM(GH).

Table 1: UV-visible and Infra-red spectral data of the DOM from saw dust and ground nut husk

λ_{max} (nm)/	**DOM**	
Infra-red frequencies (cm^{-1})	**Saw dust**	**G/nut husk**
λ_{max}	250.00	256.00
$\upsilon_{(O-H)}$ (COOH)	2959.5	2967.0
$\upsilon_{(C-H)}$ (SP^3)	2959.5	2967.9
$\upsilon_{(C=O)}$	1755.6	1722.0
$\upsilon_{(C=C)}$	-	-
$\upsilon_{(-C-O-)}$ (alcohol/phenols)	1069.7	1058.6
$\upsilon_{(\mathbf{CH_2}\ \&\ \mathbf{CH_3})}$	1408.9	1438.8
$\upsilon_{(=C-H)}$	902.0	902.0
$\upsilon_{(C-H)}$ (arene)	864.7	864.7
$\upsilon_{(O-H)}$ (phenol/alcohols)	685.8	-
$\upsilon_{(C-O-H)}$	1431.3	1438.8

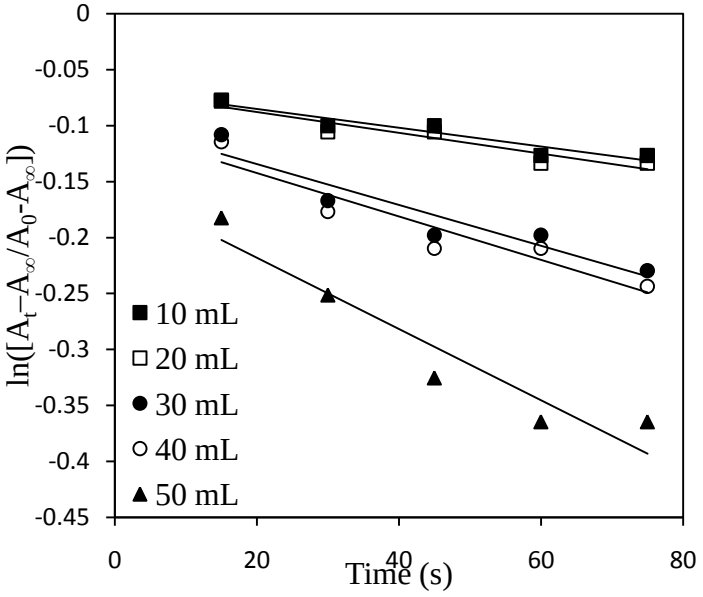

Figure 7: Plots of rate of reduction of $Cr_2O_7^{2-}$ by varying DOM (mL) obtained from GH

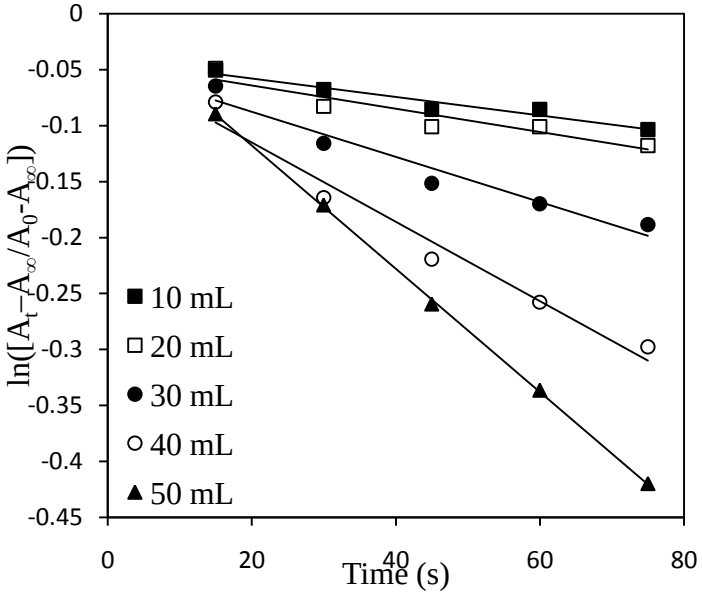

Figure 8: Plots of rate of reduction of $Cr_2O_7^{2-}$ by varying DOM (mL) obtained SD

Table 2; Pseudo-first orders, (k_{obs} and k_{pH}) data for the reduction reaction between $Cr_2O_7^{2-}$ and DOM (obtained from ground nut husk and saw dust) at varying volumes and pH

Volume (mL)	K_{obs} (s^{-1}) for $Cr_2O_7^{2-}$/DOM		pH	k_{pH} (s^{-1}) for $Cr_2O_7^{2-}$/DOM	
	G/nut husk	Saw dust		G/nut husk	Saw dust
10	0.000	0.000	2	0.003	0.004
20	0.000	0.001	4	0.001	0.003
30	0.001	0.002	6	0.001	0.001
40	0.001	0.003	8	0.000	0.001
50	0.003	0.005	10	0.000	0.000

Effect of pH on the Rate of Reduction of Cr(VI) by DOM

Figures 9 and 10 have plots for the rate of reduction of $Cr_2O_7^{2-}$ ion by DOM(GH) and DOM(SD) at varying pH, while Table 2 contains rate constant, k_{pH} values of these reactions, and the rate decrease with increase in pH. The reaction rates showed the non availability of $HCrO_4^-$ ions {the major Cr(VI) specie with the highest oxidising potential} at basic pH atleast within the period of our reaction, for the oxidation of organic matter [6, 22]. Reaction (reduction of $Cr_2O_7^{2-}$) might have taken place at such pH (8 - 10), but not reasonable enough to be detected within the 75 seconds used. Also, the major part of humic material (Fulvic acid) which is responsible for oxidation by $Cr_2O_7^{2-}$ ion is soluble over all pH, they have the highest oxygen content than others, have smaller sizes, have many –COOH and C-OH groups, making them more chemically reactive [23, 24], reaction rate was relatively low at this higher pH since there were low concentration of $HCrO_4^-$ ions and the reaction proceeded at a slow rate The rates were also higher with DOM(SD) than with DOM(GH) as reactions proceed faster when concentrations are higher.

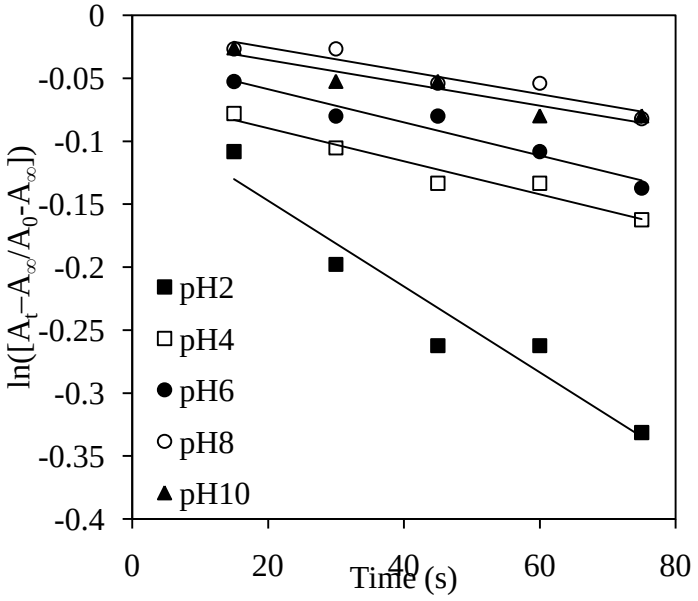

Figure 9: Effects of pH on the rates of reduction of $Cr_2O_7^{2-}$ by DOM (mL) obtained from GH

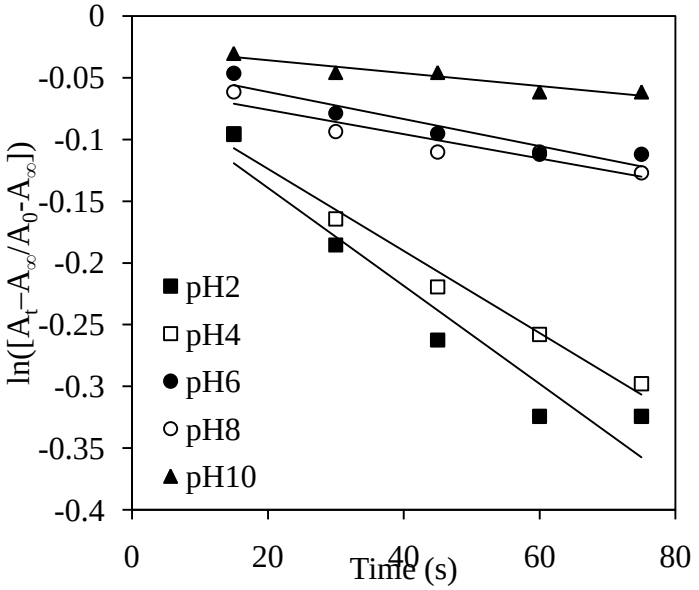

Figure 10: Effects of pH on the rates of reduction of $Cr_2O_7^{2-}$ by DOM (mL) obtained from SD

Effect of Ionic Strength on the Rate of Reduction of Cr(VI) by DOM

The reduction of $Cr_2O_7^{2-}$ ion by DOM was also monitored at varying ionic strength. Figures 11 and 12 have the plots for rate of reduction of $Cr_2O_7^{2-}$ ion by DOM(GH) and DOM(SD), while Table 3 has k_I values of the above reactions, which showed fairly constant rate with varying ionic strength. The independence of the reaction rates on

the change in ionic strength suggests that the intermediates are likely a union of two reactants ($Cr_2O_7^{2-}$and DOM(SD), DOM(GH)). The negative change in entropy of activation for the reactions (Table 6) further supports the formation of binuclear complex at the activated complex [25]. Furthermore, since the reactions are between $Cr_2O_7^{2-}$ and DOM whose ionic charge is not really established and this may, in a simple picture, cause no change in the rate constant with change in ionic strength of the reaction as it is observed in the reactions rate, Table 4 [26 and 27].

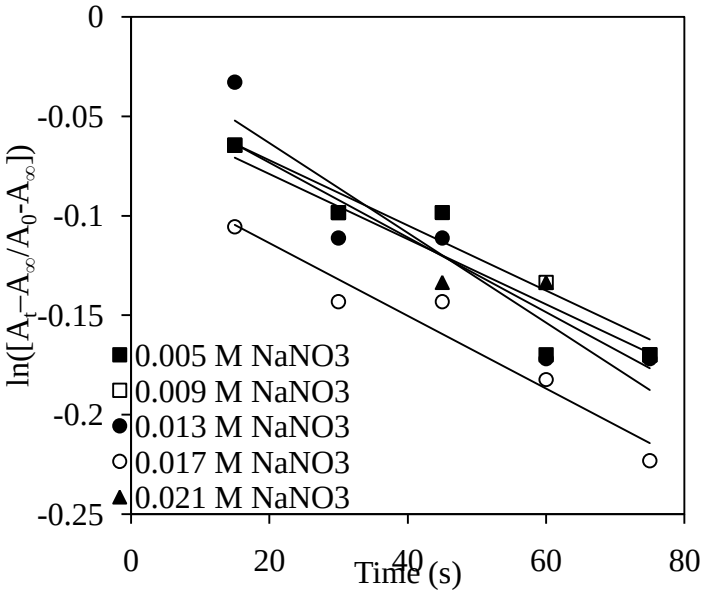

Figure 11: Effects of ionic strengths (molL^{-1}) on the rates of reduction of $Cr_2O_7^{2-}$ by DOM (mL) obtained from GH

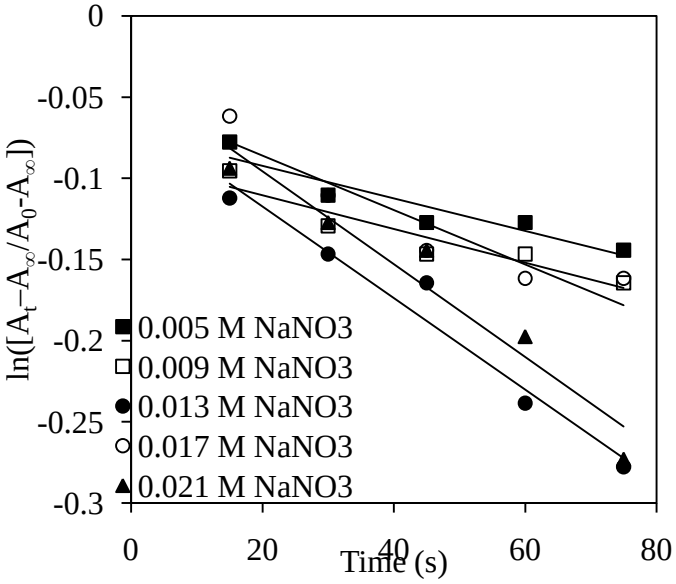

Figure 12: Effects of ionic strengths (molL^{-1}) on the rates of reduction of $Cr_2O_7^{2-}$ by DOM (mL) obtained from SD

Effects of Temperature on the Rate of Reduction of Cr(VI) by DOM

The effects of temperature on the reduction of $Cr_2O_7^{2-}$ ion by DOM showed an increase in rate as the temperature increased, Figures 13 and 14 have plots of pseudo-first order for DOM(GH) and DOM(SD) and Table 3 has the pseudo first order rate constants for these reactions but, there is no observable rate at 288 K in both cases of the DOM samples. The activation energy, Ea, enthalpy change, ΔH and entropy change, ΔS for the reduction reactions are contained in Table 6 as obtained from Arrhenius/Eyring's plots. A high E_a value signifies that the rate constant depends strongly on temperature [22], and that a slow reaction would have a high energy of activation [28].

The calculated values of activation parameters from the plots (for reduction of $Cr_2O_7^{2-}$ by DOM) gave a high energy of activation (Table 6), indicating the temperature dependence of the reduction of $Cr_2O_7^{2-}$ ion by DOM. This is not much supported by the fact that the enthalpy change for the reaction is negative indicating that the reaction is exothermic and spontaneous. Moreover, the free energy, ΔG for the reactions were found to have values in the range (-49.84992 kJmol^{-1}) at 308 K to (-71.46408 kJmol^{-1}) at 288 K, the values are indicative of the spontaneity of the reduction of $Cr_2O_7^{2-}$ ion by DOM [14 and 28]. Furthermore, the reduction of $Cr_2O_7^{2-}$ ion by DOM(GH) and DOM(SD) were considered at 0 ^oC (273 K), Figure 15. The results showed an increased reaction rate in both cases at this temperature or the reactions rates were comparable to the rate of the reactions at say 30 ^oC (303 K) – 35 ^oC (308 K), the increased reactions rates at this temperature compared to aqueous phase (or other temperatures) could likely be due to the freeze concentration effect [6]. The concentrations of DOM, protons and $Cr_2O_7^{2-}$ were high in the ice grain boundary region, which accelerated $Cr_2O_7^{2-}$ reduction. Similar, effect was noticed by Xiaoling, D. *et al*, 2014. Thus, concentrating either protons or DOM in the aqueous phase had a similar effect as carrying out the

reaction in the ice phase. Therefore, the accelerated reduction of $Cr_2O_7^{2-}$ in the ice phase could most likely be ascribed to the freeze concentration of both H^+ and DOM [6].

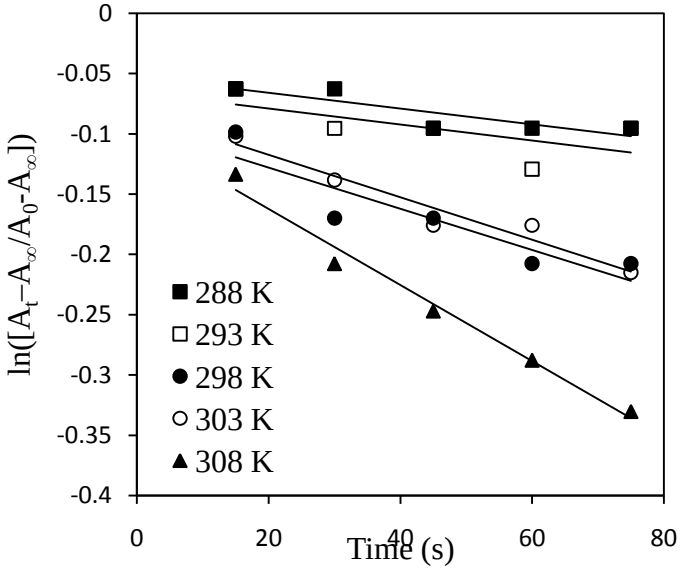

Figure 13: Effects of temperature (K) on the rates of $Cr_2O_7^{2-}$ by DOM (mL) obtained from GH

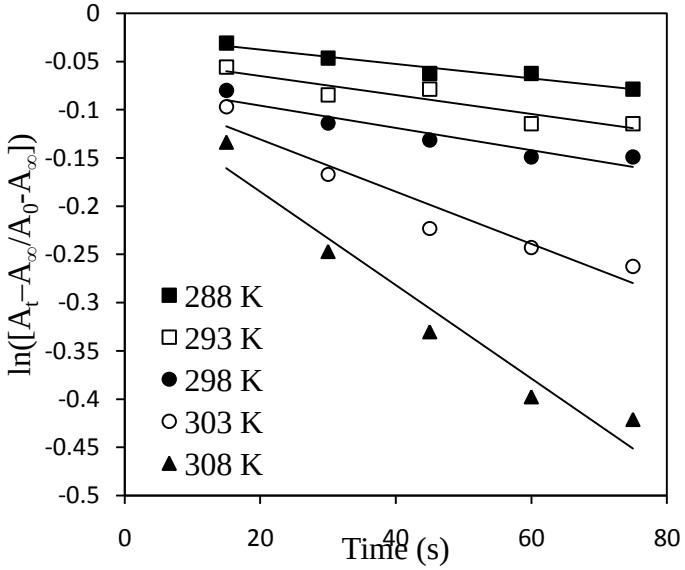

Figure 14: Effects of temperature (K) on the rates of reduction of $Cr_2O_7^{2-}$ by DOM (mL) obtained from SD

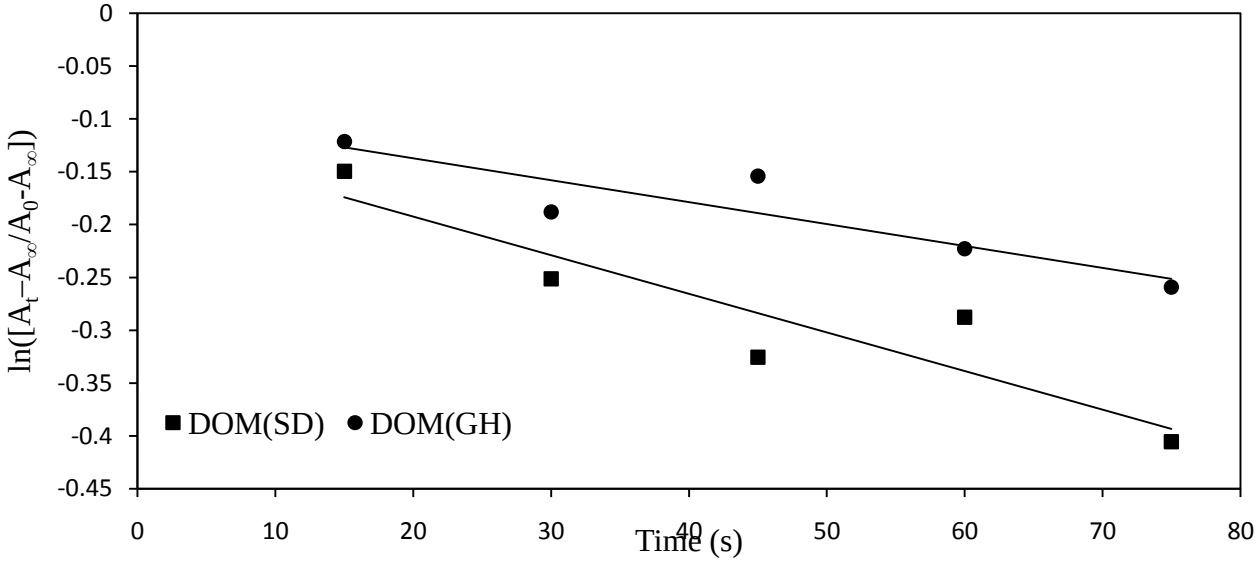

Figure 15: Plots of rate of reduction of $Cr_2O_7^{2-}$ by DOM (mL) at 273 K

Table 3: Pseudo-first orders, (k_I and k_T) data for the reduction reaction between $Cr_2O_7^{2-}$ and DOM (obtained from GH and SD) at varying ionic strengths and temperatures

I	**(mL^{-1})**	**K_{kI} (s^{-1}) for $Cr_2O_7^{2-}$/DOM**		**T**	**K_T (s^{-1}) for $Cr_2O_7^{2-}$/DOM**	
		G/nut husk	**Saw dust**	**(K)**	**G/nut husk**	**Saw dust**
0.005		0.001	0.001	273	0.002	0.003
0.009		0.001	0.001	288	0.000	0.000
0.013		0.002	0.002	293	0.000	0.001
0.017		0.001	0.001	298	0.001	0.001
0.021		0.001	0.002	303	0.001	0.002
				308	0.003	0.004

Table 4: Activation parameters (activation energy, enthalpy change and entropy change) of the reduction reactions between $Cr_2O_7^{2-}$ and DOM

Nature of Reaction	Activation Energy, Ea KJmol^{-1}	Enthalpy Change, ΔH kJmol^{-1}	Entropy Change, ΔS Jmol^{-1}K^{-1}
$Cr_2O_7^{2-}$/GH	83.31	-80.85	-32.59
$Cr_2O_7^{2-}$/SD	72.44	-69.95	-65.26

Conclusion

The reduction of $Cr_2O_7^{2-}$ ion by DOM has been reported, and the study has demonstrated that reduction of the toxic metal Cr(VI) to the less toxic form Cr(III) is feasible and fast. The use of DOM to reduce the metal ions has also given us an alternative approach (greener approach) to the prevention of environmental pollution as these agro wastes are found to lithal the environment causing one hazard and another. The DOM obtained from the agro wastes (that served as reductants) are of little or no monetary value (charge) and are obtained from renewable sources as wood is sawed frequently and ground nut is cultivated yearly in Nigeria.

References

[1]. Ramakrishnaiah, C. R. and Prathima, B. (2012). Hexavalent chromium removal from industrial watsewater by chemical precipitation method, *International Journal of Engineering Research and Applications (IJERA),* 2(2); 599-603.

[2]. Duffus, J. H. (2002). Heavy metals-a meaningless term? *International Union of Pure and applied Chemistry,* 74(5); 793–807.

[3]. Arruti, A., Fernández-Olmo, I. and Irabien, A. (2010). Evaluation of the contribution of local sources to trace metals levels in urban PM2.5 and PM10 in the Cantabria region (Northern Spain), *Journal of environmental monitoring,* 12(7); 1451–1458.

[4]. Wuana, R. A. and Okieimen, F. E. (2011). Heavy metals in contaminated soils: A review of sources, chemistry, risks and best available strategies for remediation, *International scholarly research notices, ISRN-Ecology,* 2011; 1-20.

[5]. Charalampos, V., Ifigenia, M., Ecconomou-Eliopoulos, M. and Loannis, M. (2008). "Hexavalent chromium and other toxic elements in natural waters in the Thiva – Tanagra – Malakasa Basin, Greece". *Hellenic Journal of Geoscience, 43; 57 – 66.*

[6]. Xiaoling, D., Lena, Q., Mab, J. G., Willie, H. and Yuncong, L. (2014). Enhanced Cr (VI) reduction and As (III) oxidation in ice phase: Important role of dissolved organic matter from biochar, *Journal of Hazardous Materials*, 267; 62– 70.

[7]. Adejo, S. O., Yiase, S. G., Ukoha, P. O., Iorhuna, B. T. and Gbertyo, J. A. (2014). U.Oxidation-reduction reaction of chromium(VI) and iron(III) with paracetamol: kinetics and mechanistic studies, *Archives of Applied Science Research,* 6(5); 56-67.

[8]. Shaaban, A. S., Nona-Marry, M. M. and Dimin, M. F. (2013). Characterisation of biochar derived from rubber wood sawdust through slow pyrolysis on surface porocities and functional groups, *International Tribology conference,* Malaysia, 68; 365-371.

[9]. Black, C. A. (ed.) (1965). Methods of soil analysis; Agronomy, No.9, Part 2 American Society of Agronomy, Madison, Wisconsin.

[10]. Walkley, A. and Black, I. A. (1934). An examination of the Degtjareff Method for determining soil organic matter and proposed modification of the chromic acid titration method. *Soil Science,* 37: 29-38.

[11]. Man Kee, L. and Ridzuan, Z. (2008). Production of activated carbon from saw dust using fluidised bed reactor, *International Conference on Environment, (ICENV 2008).*

[12]. Hammes, K., Smernik, R. J., Skjemstad, J. O. and Schmidt, M. W. I. (2008). "Characterisation and evaluation of reference materials for black carbon analysis using elemental composition, colour, BET surface area and ^{13}C NMR spectroscopy," *Applied Geochemistry*, 23(8); 2113–2122.

[13]. Amira, H. K., Samah, F. E. and Sherin, F. H. (2016). A review on UV spectrophotometric methods for simultaneous multicomponent analysis, *European Journal of Pharmaceutical and Medical Research*, 3(2); 348-360.

[14]. Dionisio, B., Diego, G., Jaqueline, L. P., Juliane, R. O., Karina, G. A. and Rodolfo, L. C. (2014). Kinetic and thermodynamic parameters of biodiesel oxidation with synthetic antioxidants: simplex centroid mixture design, *Journal of Brazilian Chemical Society*, 25(11); 32-40.

[15]. Ong, L. K., Kurniawan, A., Suwandi, A. C., Lin, C. X., Zhao, X. S. and Ismadji, S. (2013). Transesterification of leather tanning waste to biodiesel at supercritical condition: Kinetics and thermodynamics studies, *The Journal of Supercritical Fluids*, 75; 11–20.

[16]. Cheong-Song, C., Jin-Woo, K., Cheol-Jin, J., Huiyong, K. and Ki-Pung, Y. (2011). Transesterification kinetics of palm olein oil using supercritical methanol, *The Journal of Supercritical Fluids*, 58(3); 365–370.

[17]. Helal, A. Aly., Murad, G. A. and Helal, A. A. (2011). Characterisation of different humic materials by various analytical techniques, *Arabian Journal of Chemistry*, 4(1); 51-54.

[18]. Shie-Jie, G., Chen, Z., Zong-Hai, S., Jun, Z., Jian-Guo, L. and Jun-Qing, L. (2016). Spectroscopic characteristics of dissolved organic matter in afforestation forest soil of Miyun District, Beijing, *Journal of Analytical Methods in Chemistry*, 5; 56-62.

[19]. Silverstein, R. M., Webster, F. X. and Kiemle, D. J. (2005). *Spectrometric identification of organic compounds*, John Wiley and Sons International, 7th Ed., 72-126.

[20]. Shamshad, K., Wu, Y., Zhang, X., Liu, J., Sun, J. and Hu, S. (2014). Estimation of concentration of dissolved organic matter from sediment by using UV–visible spectrophotometer, *International Journal of Environmental Pollution and Remediation*, 2(1); 24-29.

[21]. Atkins, P. and De paula, J. (2000). *Physical phemistry.* Oxford University Press. New Delhi, 7th Ed., 960-62.

[22]. Cotton, F. A. and Wilkison, G. (1978). *Advanced inorganic chemistry; A comprehensive text.* Wiley Eastern Ltd, New Delhi, 3rd Ed., 818-870.

[23]. Martina, K. and Miloslav, P. (2005). Solubility and dissociation of lignitic humic acids in water suspension, *Colloids and Surfaces A: Physicochemical and Engineering Aspects*, 252(2-3); 157-163.

[24]. Kipton, H., Powell, J. and Town, R. M. (1992). Solubility and fractionation of humic acid; effect of pH and ionic medium, *Analytica Chimica Acta*, 267(1); 47-54.

[25]. Ukoha, P. O. and Ibrahim, E. (2004). Mechanism of the oxidation of β-mercaptoacetic acid by trioxoiodate in aqueous acid medium, *Chemclass Journal*. Pp 55-58.

[26]. Kumar, P. (2013). Study of effect of variation of ionic strength of the medium on velocity constant of Ru(III) catalysed oxidation of hydroxyl benzoic acids by chloramine-T in acidic medium, *Oriental Journal of Chemistry*, 29(4);23-28.

[27]. Hughes-Jones, N. C., Gardner, B. and Telford, R. (1964). The effect of pH and ionic strength on the reaction between anti-D and erythrocytes, *Immunology*, 7; 72-81.

[28]. Cantu, Y., Remes, A., Reyna, A., Martinez, D., Villarreal, J., Ramos, H., Trevino, S., Tamez, C., Martinez, Eubanks, T. and Parsons, J. G. (2014). Thermodynamics, kinetics, and activation energy studies of the sorption of chromium(III) and chromium(VI) to a Mn_3O_4 nano material, *Chemical Engineering Journal*, 254(15); 374-383.